Stage-specific expression patterns and co-targeting relationships among miRNAs in the developing mouse cerebral cortex

Hristo Todorov[1], Stephan Weißbach[1,2], Laura Schlichtholz[1,3], Hanna Mueller[1], Dewi Hartwich[1], Susanne Gerber[*1], Jennifer Winter[*1,4]

[1] Institute of Human Genetics, University Medical Center of the Johannes Gutenberg University Mainz, Germany

[2] Institute of Developmental Biology and Neurobiology (iDN), Johannes Gutenberg University, Mainz, Germany

[3] Focus Program of Translational Neurosciences, University Medical Center Mainz, Mainz, Germany

[4] Lead contact: Jennifer Winter

[*] Corresponding authors: Susanne Gerber and Jennifer Winter

Contact data

Hristo Todorov: hristo.todorov@uni-mainz.de

Stephan Weißbach: s.weissbach@uni-mainz.de

Laura Schlichtholz: schlichtholz.laura@googlemail.com

Hanna Mueller: hanna.mueller.1909@gmail.com

Dewi Hartwich: dewi.hartwich@unimedizin-mainz.de

Susanne Gerber: sugerber@uni-mainz.de

Jennifer Winter: jewinter@uni-mainz

Keywords

Embryonic cortical development, miRNAs, co-targeting networks, gene silencing

Abstract

microRNAs are particularly important during brain development, however, the composition and temporal dynamics of miRNA regulatory networks are not sufficiently characterized. Here, we performed small RNA sequencing of mouse embryonic cortical samples at E14, E17, and P0 as well as in neural progenitor cells differentiated *in vitro* into neurons. Using co-expression network analysis, we detected clusters of miRNAs that were co-regulated at distinct developmental stages. miRNAs such as miR-92a/b acted as hubs during early, and miR-124 and miR-137 during late neurogenesis. Notably, validated targets of P0 hub miRNAs were enriched for down-regulated genes related to stem cell proliferation, negative regulation of neuronal differentiation and RNA splicing, among others, suggesting that miRNAs are particularly important for modulating transcriptional programs of crucial factors that guide the switch to neuronal differentiation. As most genes contain binding sites for more than one miRNA, we furthermore constructed a co-targeting network where numerous miRNAs shared more targets than expected by chance. Using luciferase reporter assays, we demonstrated that simultaneous binding of miRNA pairs to neurodevelopmentally relevant genes exerted an enhanced transcriptional silencing effect compared to single miRNAs. Taken together, our study provides a comprehensive resource of miRNA longitudinal expression changes during corticogenesis. Furthermore, we highlight several potential mechanisms through which miRNA regulatory networks can shape embryonic brain development.

Introduction

Mammalian brain development is an extraordinarily complex process where neural progenitor cells proliferate and give rise to all neuronal and glial cell types. Numerous transcriptional,

51 post-transcriptional, and epigenetic mechanisms integrate with each other to control progenitor
52 proliferation and self-renewal, differentiation, and lineage commitment as well as migration in
53 a strictly spatio-temporal manner. One of the key regulators of these processes are microRNAs
54 (miRNAs). In most cases, these small RNAs bind to their target mRNAs' 3'- untranslated
55 region (3'UTR) to induce mRNA degradation or translational inhibition. In the canonical
56 pathway, miRNA genes are transcribed into a pri-miRNA in the cell nucleus by PolII/III (1, 2).
57 In subsequent processing steps, the pri-miRNA is cleaved into a hairpin pre-miRNA by the
58 microprocessor complex Drosha-Dgcr8 and transported to the cytoplasm by Exportin-5 (3-6).
59 In the cytoplasm, the pre-miRNA is bound and cleaved by a complex containing the RNase
60 Dicer1 to form the mature miRNA duplex (7). From this duplex, the functional strand is loaded
61 into the RISC complex, guiding it to the 3'UTR's target site (8). Mice carrying conditional
62 *Dicer* gene deletions in the embryonic telencephalon have shown a variety of phenotypes in
63 the cerebral cortex, such as reduced cell proliferation and impaired neuronal differentiation,
64 increased apoptosis, defective cortical layering and microcephaly (9-14).
65 In the brain, 70% of all miRNAs are expressed, most of them in a highly cell-type- and
66 developmental-time-specific manner (15). Given that the total number of human miRNAs is
67 estimated to be ~ 2300, at least 1600 different miRNAs may be expressed in the brain (16).
68 While this suggests that miRNA regulation is generally important for brain development and
69 function, the specific functions of most miRNAs remain unknown. Single miRNAs are
70 involved in some of these processes including, for example, cell proliferation (e.g. let-7, miR-
71 124, miR-9), neuronal differentiation (e.g. let-7, miR-124, miR-9, miR-128) and migration
72 (e.g. miR-9, miR-124, miR-379-410) (17, 18). Many of the functionally studied miRNAs are
73 among the most highly expressed in the brain such as miR-9, miR-124 and let-7 (17). Most
74 miRNAs typically have a relatively weak effect on their target genes (19, 20). Previous research
75 has suggested that the regulatory potential of a given miRNA could be enhanced by cooperating

with other miRNAs in co-targeting networks (21). This hypothesis is supported by the fact that most 3'UTRs contain more than one miRNA binding site and most miRNAs have matching binding sites in up to several hundred 3'UTRs. A network of miRNAs co-operatively binding at distinct 3'UTR positions can potentially enhance target gene repression by additive or synergistic effects (22, 23). MiRNA binding at closely spaced binding sites (~15 – 35 nt) can further enhance the repressive effect (23-25). We and others have previously identified mRNAs that are targeted by several miRNAs leading to a synergistic or additive repressive effect (19, 20, 26). For example, miRNAs of the miR-379-410 cluster regulate neurogenesis by targeting multiple miRNA binding sites in the N-cadherin 3'UTR in an additive manner (19). While this highlights the regulatory potential of such miRNA networks during brain development, their detailed composition and temporal dynamics remain poorly characterized. Using an unbiased bioinformatics approach to identify co-targeting networks in mouse tissues, Cherone and colleagues recently found that miRNAs enriched in the human prefrontal cortex had more co-targeting partners than those enriched in other tissues suggesting that miRNA co-targeting is especially important in the brain (20).

In the current study, we employed high-throughput small RNA sequencing of the mouse cerebral cortex to create a detailed map of miRNA expression patterns and their longitudinal dynamics at key developmental stages. Using miRNAs whose expression was significantly correlated with developmental time, we constructed a comprehensive co-targeting network in which miRNAs with higher expression levels were associated with significantly more co-targeting relationships. In luciferase assays, we validated the enhanced gene silencing effect of cooperative miRNA binding in a set of target genes involved in the regulation of nervous system development.

Results

101 ***Temporal dynamics of miRNA expression during cerebral cortex development***

102 To study the expression patterns of miRNAs during mammalian corticogenesis, we performed
103 small RNA sequencing in both female and male mice at a progenitor-dominated developmental
104 phase (embryonic day E14), at an intermediate time point (E17) and at birth (postnatal day P0)
105 when neurons from all six layers of the neocortex have been born (27, 28) (Fig 1A). Using
106 stringent filtering criteria for expression levels (>10 CPM in at least five samples), we detected
107 a total of 489 miRNAs with only 13 of those corresponding to novel miRNAs. In agreement
108 with previous reports (17, 29), miR-9, members of the let-7 family, miR-128, and miR-124
109 were among the top 20 most abundantly expressed miRNAs in the developing cerebral cortex
110 (Fig S1). Principal component analysis (PCA) revealed a distinct separation of samples
111 according to the developmental stage. However, E17 and P0 samples had a more similar global
112 expression pattern to each other compared to E14 (Fig 1B). Since we did not observe apparent
113 differences related to sex, female and male samples were processed together in the subsequent
114 analyses.

115 We detected the highest number of differentially expressed miRNAs in the E14 vs. P0 time
116 points, where 169 miRNAs were up- and 172 were downregulated (Fig 1C-G). However, the
117 major transcriptional shift already occurred in the transition from E14 to E17, where approx.
118 57% of all detected miRNAs significantly changed their expression level (122 up- and 144
119 down-regulated miRNAs). In contrast, only 36% of all detected miRNAs were differentially
120 expressed in E17 vs. P0 samples (82 up-regulated and 93 down-regulated miRNAs).
121 Interestingly, a higher number of miRNAs were consistently down-regulated at earlier
122 developmental time-points in all pairwise comparisons (45 vs. 32 up-regulated miRNAs, Fig
123 1C, D, H).

124 To study the expression of miRNAs specifically during neurogenesis, we isolated NPCs from
125 the cortices of mouse embryos at E14 and differentiated them *in vitro* into neurons. Small RNA

126 sequencing of these cells revealed 110 miRNAs that were up-regulated and 113 miRNAs that
127 were down-regulated in NPCs compared to neurons, respectively. miR-124-3p and miR-369-
128 3p were the most significantly up-regulated miRNA in neurons, whereas miR-155-3p and miR-
129 34b-3p were the most significantly up-regulated miRNAs in NPCs (Fig S2A, D). 66% of the
130 up-regulated (72 out of 110) and 65% of the down-regulated (73 out of 113) miRNAs in NPCs
131 vs. neurons were also differentially expressed in the comparison of bulk samples from E14 vs.
132 P0, confirming the replicability of the expression patterns we observed (Fig S2B-D).
133 Interestingly, these overlapping miRNAs corresponded to 43% of all up-regulated and 42% of
134 the down-regulated miRNAs in E14 vs. P0, suggesting that a large proportion of the
135 differentially regulated miRNAs might be attributable to the non-neuronal cells in the bulk
136 samples. This observation is plausible, as gliogenesis takes place roughly between E17 and P0
137 of cortical development (28, 30) therefore the bulk samples from P0 likely contained both
138 neuronal and non-neuronal cell types.
139

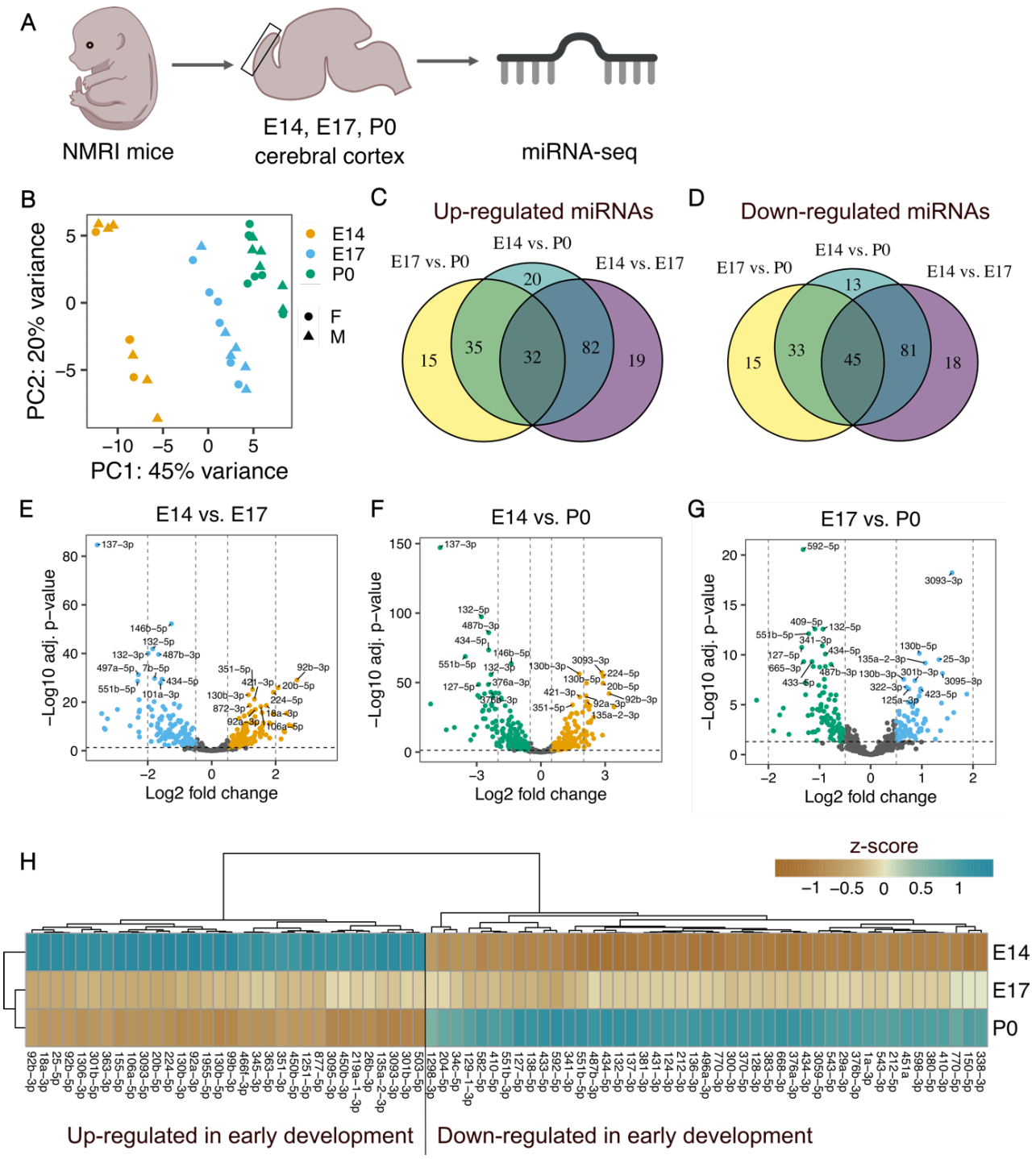

Fig. 1. Expression changes of miRNAs during mouse cerebral cortex development. A Schematic representation of the experimental approach. **B** Principal component analysis of small RNA sequencing samples from the cerebral cortex of female and male mice at different developmental stages. **C** Venn-diagram of up-regulated miRNAs at earlier compared to later developmental stages. **D** Venn-diagram of down-regulated miRNAs at earlier compared to later developmental stages. **E-G** Volcano plots of differentially expressed miRNAs. Positive log2 fold changes indicate miRNAs up-regulated at earlier

147 compared to later developmental stages in each pairwise comparison (E14 vs. E17, E14 vs. P0 and E17
148 vs. P0). **H** Heatmap of miRNAs differentially expressed in each pairwise comparison of different
149 developmental stages. Mean expression values per developmental stage are shown as z-scores.
150

151 ***Weighted co-expression gene network analysis identifies sets of co-regulated miRNAs***
152 ***during the development of the cerebral cortex***

153 Next, we applied weighted co-expression gene network analysis (WCGNA) to construct
154 networks of co-expressed miRNAs and better characterize their transcriptional dynamics along
155 the cortical developmental trajectory. We obtained 18 modules that were assigned to arbitrary
156 colors (Fig 2A). Module eigengenes (MEs) that correspond to the first dimension in a principal
157 component analysis of the expression matrix of the corresponding WCGNA module, served as
158 proxies for the characteristic transcriptomic signature of each module. Six MEs were
159 significantly negatively correlated with the developmental time point indicating that the
160 miRNAs in the respective modules showed overall reduced expression levels at later compared
161 to earlier developmental stages (Fig 2B). In contrast, four modules contained miRNAs whose
162 eigengene expression significantly increased during brain development. The black module,
163 which contained the highest number of miRNAs (139), had the strongest negative correlation
164 with the developmental stage. The overall expression pattern captured by the ME, indicated
165 that the black module contained miRNAs whose expression level peaked at E14 and dropped
166 at E17, remaining stable afterwards (Fig 2C). The green module was the second largest,
167 containing 101 miRNAs with generally linearly increasing expression levels from E14 to P0
168 (Fig 2D). Remarkably, although these two modules were regulated in opposite directions, they
169 shared most of their targets (6244 common targets, corresponding to 79% of all black module
170 and 72% of all green module targets, Fig S3C). Gene ontology analysis using the genes targeted
171 by the miRNAs revealed that both the black and the green modules are involved in the

172 regulation of key nervous system developmental processes such as axon development and

173 guidance, neuron projection, dendrite development, and synapse organization (Fig 2E, F).

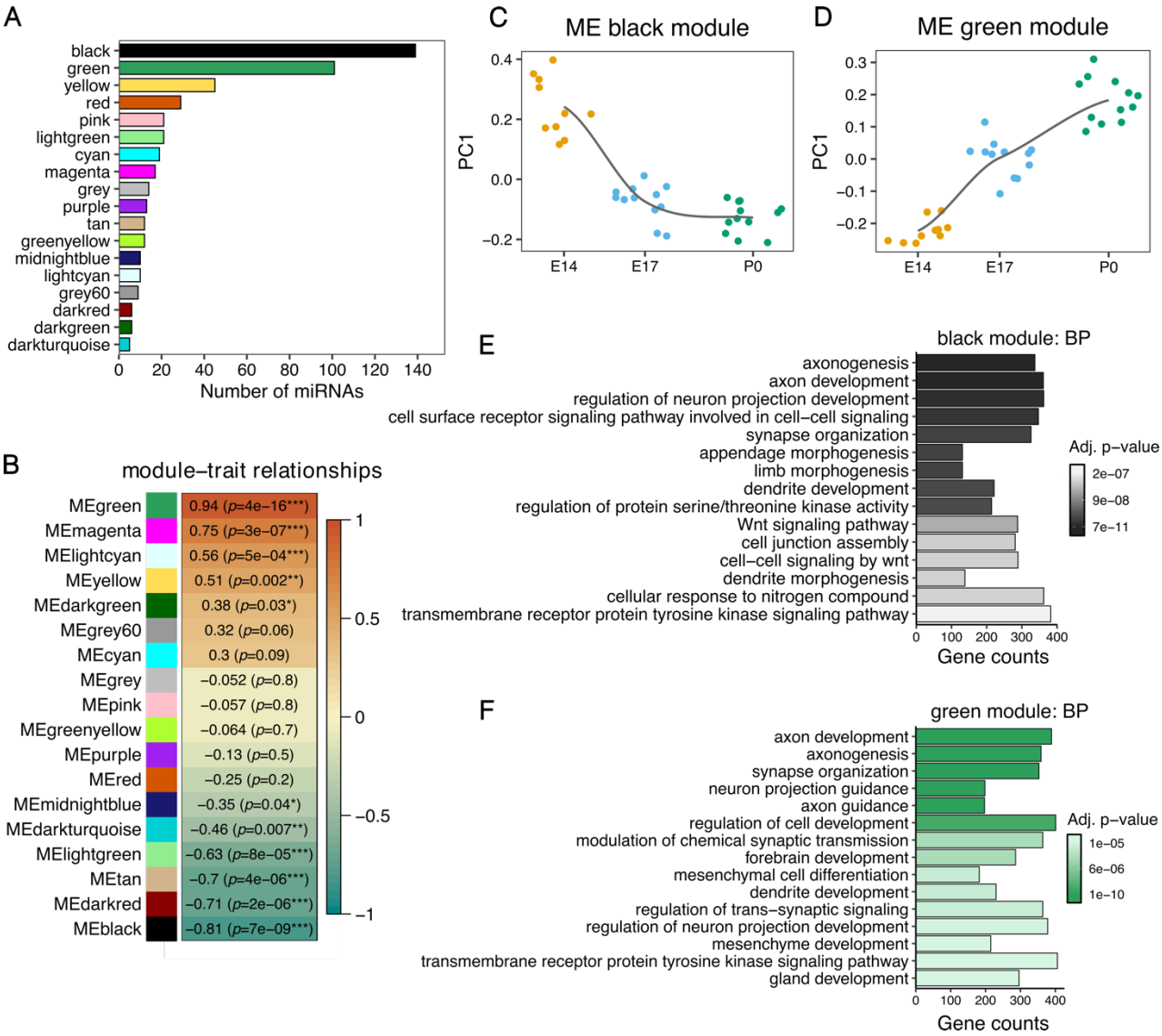

174

175 **Fig. 2 Weighted miRNA co-expression analysis. A** Bar plot showing the number of miRNAs in each

176 co-expression network module. **B** Pearson correlation between developmental stages of the mouse

177 cerebral cortex (E14, E17 and P0) and the module eigengenes (ME). ***p<0.001, ** p<0.01, *p<0.05.

178 **C-D** Module eigengene values at each developmental stage for the black and green module. **E-F** Top

179 15 enriched GO terms for the biological process (BP) category for the gene targets of the black and

180 green modules.

181 To identify key miRNAs at early and late embryonic brain developmental stages, we

182 reconstructed the network structure of miRNAs within the black and green modules and

183 identified key driver (hub) miRNAs as described previously (31, 32). The black module
184 contained 21 hub miRNAs. 12 miRNAs were also up-regulated in NPCs compared to neurons
185 including members of the miR-92 family - miR-92a, miR-92b (Fig 3C). Moreover, we detected
186 18 key driver miRNAs in the green module. Ten of these were also significantly up-regulated
187 in neurons compared to NPCs, including the neuron-specific miR-124 and miR-137 (Fig 3D).
188 This analysis confirmed the stage-specific regulation of a core set of miRNAs during
189 embryonic cortical development.
190 Importantly, all hub miRNAs in the green module and all but one miRNA in the black module
191 were significantly differentially regulated in the E14 compared to the P0 developmental stage
192 (Fig 3A, B). Furthermore, hub miRNAs in both the black and the green modules showed
193 significantly stronger module membership and gene trait significance estimates compared to
194 the remaining miRNAs in the respective module (Fig S3E-H), thereby confirming their
195 importance. Here, module membership corresponds to the correlation between the miRNA's
196 expression and the module eigengene. Furthermore, the gene trait significance represents the
197 correlation between miRNA expression and the trait of interest, in our study – the
198 developmental stage (33).
199 To gain an insight into the relevance of hub miRNAs in regulating target gene expression across
200 development, we re-analyzed RNA-seq data from the mouse cortex at E14.5, E16.5 and P0
201 from the study by Weyn-Vanhentenryck and colleagues (34). We limited this analysis to the
202 experimentally validated targets of the conserved hub miRNAs that we obtained from
203 miRTarBase (35). We did not observe a significant deviation in the differential expression of
204 target genes of the black module when comparing P0 and E14.5 (Fig 3E). This could likely be
205 explained by the overall lower number of validated targets for conserved key driver miRNAs
206 from the black module (Fig S3D). However, the number of down-regulated targets of the green
207 module's hub miRNAs was significantly higher compared to the overall background

208 distribution of differentially expressed genes (Fig 3E). The increased proportion of genes with
209 a reduced expression at the time point when the green module's hub miRNAs that target them
210 have their expression peak strongly suggests that these miRNAs are involved in repressing
211 these targets' expression *in vivo*.
212 To gain insight into the biological processes that the down-regulated targets of green module
213 hub miRNAs are involved in, we performed a GO annotation analysis (Fig 3F). Notably, many
214 of these genes are associated with the cell cycle, stem cell maintenance and proliferation (e.g.,
215 the transcription factors *Sox2, Sox9* and *Sox11),* cell fate commitment (e.g., *Neurog2),* and
216 negative regulation of neuronal differentiation. Furthermore, several targets are involved in
217 activating the Notch signaling pathway (e.g., *Notch1, Notch3)* and negatively regulating the
218 Wnt pathway. Important mediators of RNA splicing (e.g., the RNA binding proteins *Ptbp1* and
219 *Ptbp2)* were also among the down-regulated targets. Notably, the green module hub miR-124-
220 3p is known to repress *Ptbp1* expression and thereby induce neuron-specific alternative
221 splicing programs required for neuronal differentiation (36). Therefore, these results indicate
222 that miRNAs might be particularly important for the switch from undifferentiated NPCs to
223 differentiated neurons by silencing the expression of key factors that promote stem cell
224 maintenance, proliferation and non-neuronal splicing patterns.

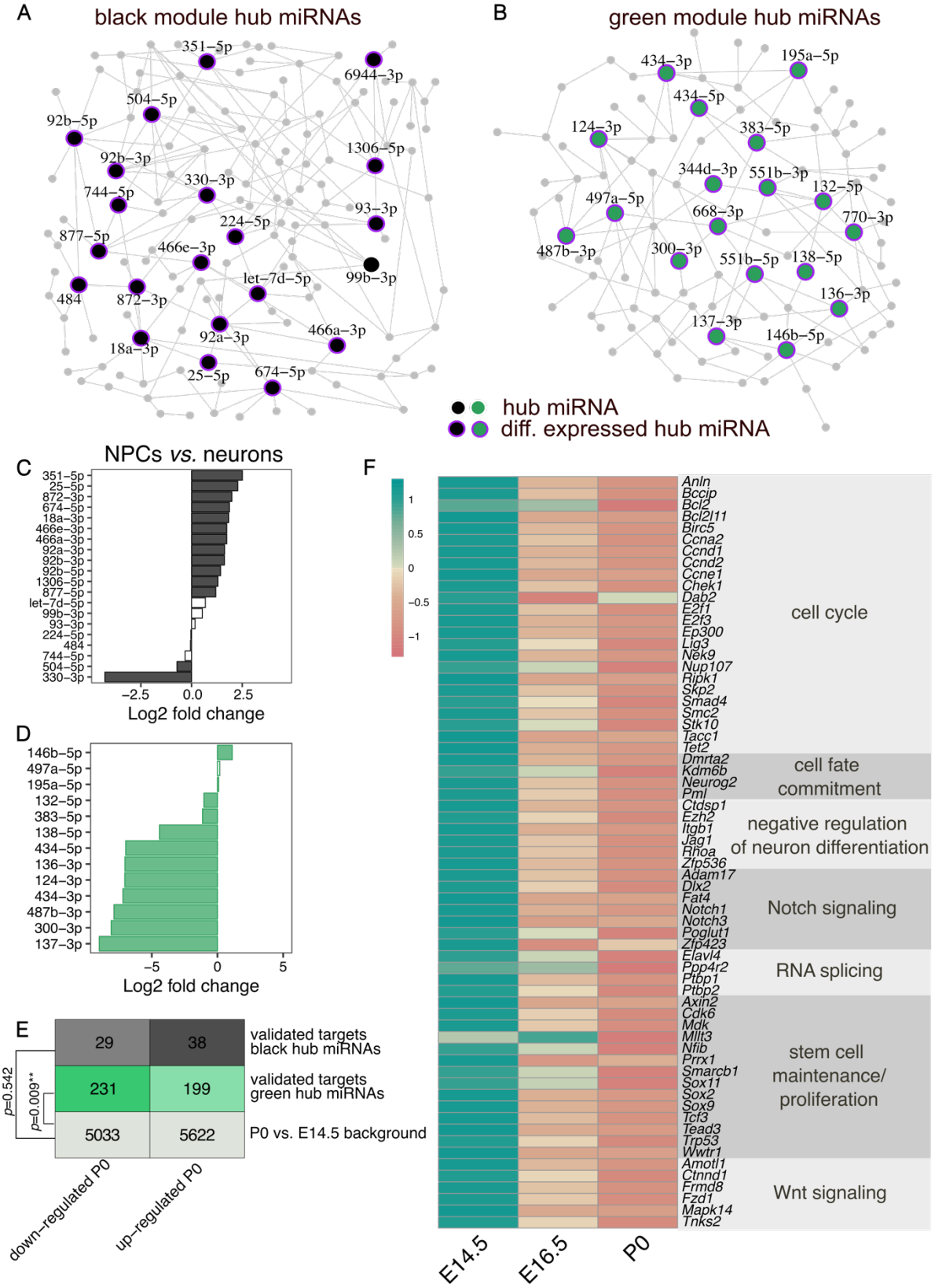

225

226 **Fig. 3 Hub miRNAs in the black and green modules.** Network plot showing the hub miRNAs in the

227 black **(A)** and green **(B)** modules. Hub miRNAs are represented as bigger nodes. Purple halos around

228 the nodes indicate miRNAs that are significantly differentially expressed between E14 and P0. **C-D**
229 Differential expression of hub miRNAs from the black **(C)** and green **(D)** module detected in the NPCs
230 versus neurons analysis. Positive log2 gold changes indicate an up-regulation in NPCs, negative values
231 correspond to up-regulation in neurons. White bars indicate non-significant fold changes. **E** Distribution
232 of differentially expressed genes in the mouse cerebral cortex between E14.5 and P0. The overall
233 number of genes as well as the number of these genes that are validated targets from miRNAs in the
234 black and green module as obtained from miRTarBase are given. The comparison of the distribution of
235 differentially expressed targets of the black or green module from the overall distribution of
236 differentially expressed genes was performed with a Fisher's exact test. **F** Z-score transformed average
237 expression of selected validated targets of miRNAs from the green module that are significantly up-
238 regulated at E14.5 compared to P0. The expression values in E and F were obtained from the study by
239 Weyn-Vanhentenryck et al. (34).
240

241 ***Prediction of miRNA co-targeting networks in the developing cerebral cortex***

242 WCGNA revealed that clusters containing multiple miRNAs are co-expressed during cortical
243 development. Furthermore, when looking at the predicted targets of the black and green
244 modules, we observed that only approx. 30% were potentially targeted merely by a single
245 miRNA. On average, each gene was associated with more than 3 miRNAs (Fig S3A-B). This
246 apparent redundancy of simultaneously expressed miRNAs that putatively bind to overlapping
247 sets of genes supports the previously proposed hypothesis that miRNAs might act together to
248 co-operatively exert stronger gene silencing. To construct a comprehensive co-targeting
249 network of miRNAs in the developing cerebral cortex, we designed a statistical framework that
250 allowed us to detect which miRNAs share significantly more targets than expected by chance.
251 In this analysis, we included all miRNAs whose module eigengene was correlated significantly
252 with developmental time in the WCGNA (Fig 2B). Furthermore, we only considered conserved
253 miRNAs with at least 300 conserved targets and distinct seed sequences (20). miRNAs

254 belonging to the same broad conserved family and thereby having identical seed sequences,
255 were grouped together for the statistical testing. After applying these filtering criteria, we
256 performed the co-targeting prediction with a set of 77 miRNA families corresponding to 106
257 individual miRNAs (Fig 4A). We detected 1216 significant co-targeting pairs with an adjusted
258 p-value <0.05 (Fig 5) and each miRNA had on average 41 co-targeting relationships (Fig 4B).
259 Interestingly, the number of significant co-targeting relationships was positively correlated
260 with the miRNA's average expression level (Fig 4C). This finding implies that important
261 miRNAs might need to be produced at higher amounts to facilitate their involvement in
262 multiple cooperative gene silencing interactions in the co-targeting network. Importantly, hub
263 miRNAs such as mir-92a/b from the black module as well as miR-124 and miR-137 from the
264 green module were among the miRNAs with the highest expression level and highest number
265 of co-targeting relationships (Fig 4C) indicating that these miRNAs might be master regulators
266 in both co-expression and multi-targeting networks. As expected, the length of the 3' UTR was
267 positively correlated with the number of significant miRNA pairs targeting a gene (Fig 4D).
268 Interestingly, *Nova1*, was among the top 10 genes involved in the highest number of co-
269 targeting associations. NOVA1 is a neuron-specific splice factor that is crucial for neuronal
270 viability (37) and regulates the alternative splicing of genes involved in synapse formation (38).
271 In line with this, we detected a significant *Nova1* expression increase in cortical samples at P0
272 compared to E14.5 (log2 fold change = 0.84, adj. p-value <0.0001) when re-analyzing the
273 RNA-seq data from Weyn-Vanhentenryck et al. (34). Thus, our findings further highlight the
274 potential importance of miRNAs in regulating neurodevelopment by influencing the
275 expression of crucial effectors of alternative splicing processes.
276 Remarkably, we detected the strongest co-targeting relationship between miR-137 and the
277 miR-25/miR-363/miR-92 family, sharing 353 common gene targets (Fig 4F). While miR-137
278 was up-regulated at later developmental stages, all members of the miR-25/miR-363/miR-92

279 cluster were regulated in the opposite direction. This prominent association between hub
280 miRNAs, that were not co-expressed, prompted us to investigate the distribution of intra-
281 modular (between miRNAs from the same module) and inter-modular (miRNAs from different
282 modules) co-targeting relationships for the black and green WCGNA modules. While we
283 expected that relationships between co-expressed miRNAs might be enriched, we indeed
284 observed a comparable distribution of intra- and inter-modular co-targeting pairs (Fig 4E).
285 These findings point to two distinct potential regulatory mechanisms justifying the need for
286 miRNAs to share significantly more targets than expected by chance. On the one hand,
287 miRNAs with common targets regulated in opposite directions during cortical development
288 might arise from the need to facilitate target gene regulation at different time points or in
289 distinct cell types. On the other hand, co-expressed miRNAs that regulate the same genes could
290 cooperatively bind to their targets to exert a stronger repressive effect compared to single
291 miRNAs.
292

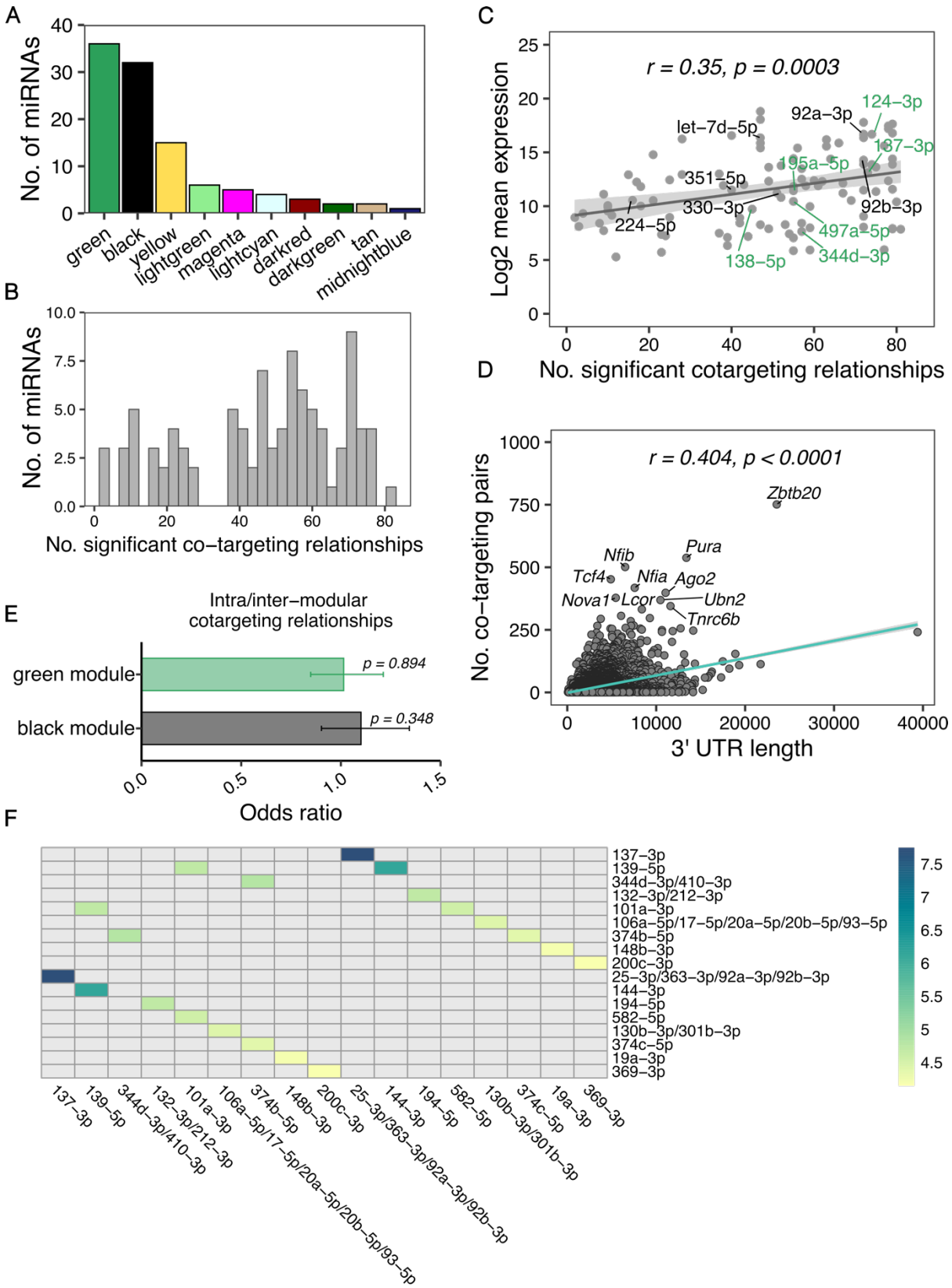

293

294 **Fig. 4. Features of the miRNA co-targeting network of the developing cerebral cortex. A** Bar plot
295 showing the number of miRNAs from each module that were included in the co-targeting analysis after
296 applying the filtering criteria. **B** Histogram of the number of miRNAs having a specific number of

297 significant co-targeting relationships. **C** Scatter plot indicating the correlation between the number of
298 co-targeting relationships with the log2-transformed miRNA's average expression level; *r* corresponds
299 to Pearson's correlation coefficient. Labels indicate hub miRNAs from the WCGNA analysis of the
300 black and green modules **D** Correlation between the 3' UTR length of target genes and the number of
301 significant co-targeting miRNA pairs the genes are targeted by; *r* corresponds to Pearson's correlation
302 coefficient. **E** Bar plot with the association of the number of intra-modular (between miRNAs of the
303 same module) and inter-modular (involving miRNAs from different modules) co-targeting
304 relationships. Odds ratios were obtained with a Fisher's exact test. Error bars indicate the 95%
305 confidence interval. **F** Heatmap with the top 10 strongest co-targeting relationships between pairs of
306 miRNAs/conserved miRNA families. Values indicate odds ratios as measures of association between
307 the co-targeting pairs.
308

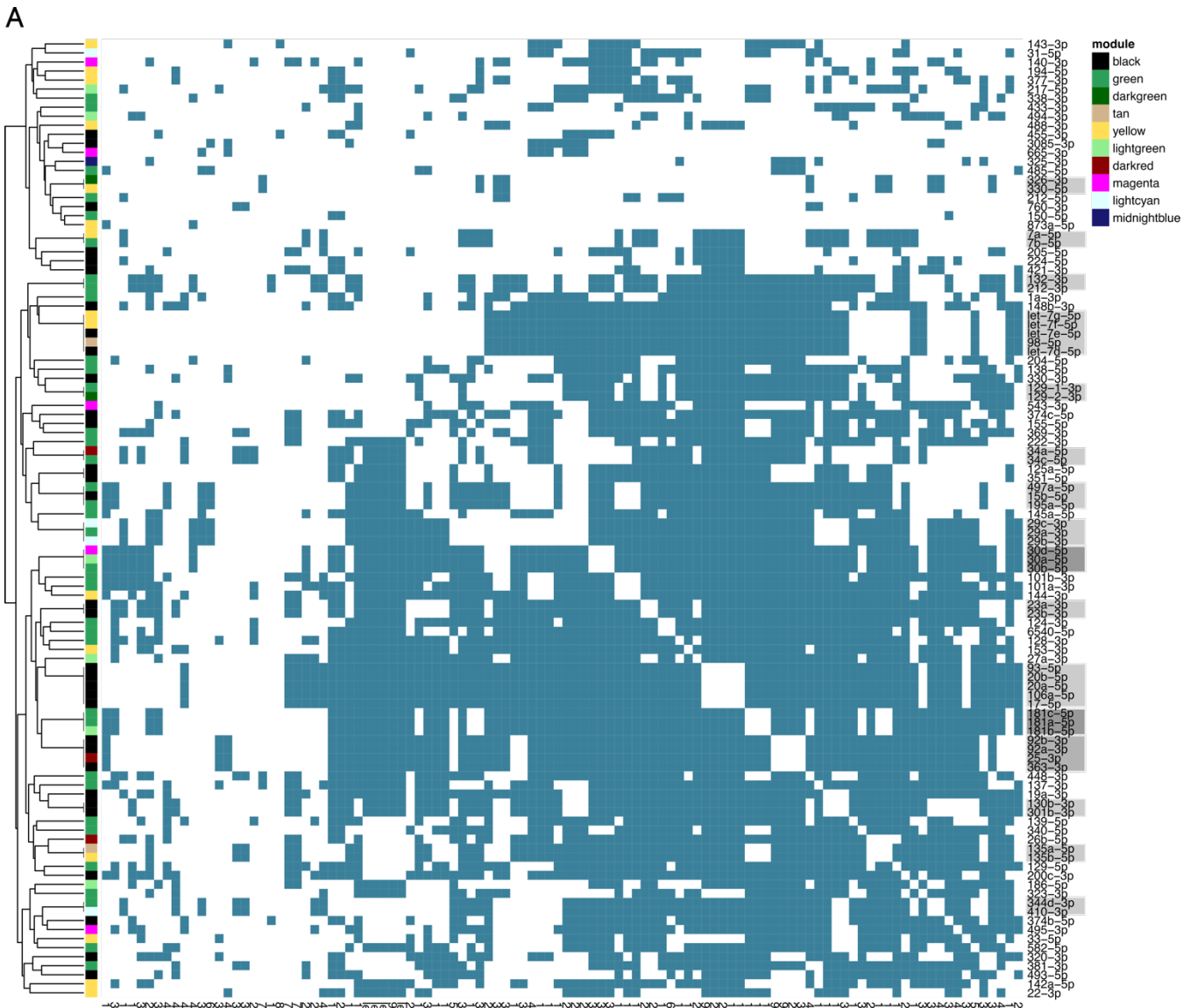

Fig. 5 Significant co-targeting miRNA pairs. Colored squares on the heatmap indicate significant co-targeting relationships. miRNAs that belong to the same conserved family and therefore have identical co-targeting relationships to each other, are indicated with gray rectangles on the vertical axis of the heatmap.

Enhanced gene silencing effect by cooperative binding of co-expressed miRNAs

To validate the hypothesis that co-expressed miRNAs bind co-operatively to their common targets to enhance their repressive effect, we employed luciferase reporter assays focusing on miRNAs that were up-regulated during embryonic brain development. We performed a gene

319 ontology term look-up of all targets and filtered potential candidate genes for terms including
320 brain/forebrain development and (central) nervous system development. Then we looked for
321 genes with two or more conserved binding sites in their 3' UTR for miRNAs up-regulated
322 during cortical development. Using this strategy, we compiled a list of 7 candidate target genes
323 (*Neurod1, Apc, Dcx, Ndst1, Zeb2, Src* and *Cxcl12*) and 5 miRNAs (miR-128-3p, miR-129-5p,
324 miR-135b-5p, miR-137-3p and miR-153-3p).
325 First, we performed RT-qPCR analyses to validate the expression patterns that we observed in
326 the bulk sequencing of the miRNAs selected for luciferase assays. All 5 miRNAs showed
327 significantly increased expression levels in neurons compared to NPCs with mean relative
328 quantification (RQ) values ranging from 2.9 to 3987 in the case of miR-135b-5p (Fig S4A-E).
329 Furthermore, all miRNAs were associated with increased expression at later developmental
330 stages in cortical tissue samples. The relative expression of miR-128-3p and miR-135b-5p
331 significantly increased over all time points analyzed (Fig S4 F, H). miR-137-3p and miR-153-
332 3p were associated with a significantly higher expression levels at E17 and P0 compared to
333 E14 (Fig S4 I, J). miR-129-5p was the only miRNA that showed a non-significant trend of
334 higher expression at later developmental stages (Fig S4G).
335 Subsequently, for each luciferase reporter assay, we cloned the target gene's 3'UTR fragment
336 containing the binding sites of the selected miRNAs, downstream of the synthetic *Renilla*
337 luciferase gene into the psiCHECK^{TM}-2 vector, which also expresses firefly luciferase as
338 internal control. Plasmids were then co-transfected into HEK293 cells with different
339 combinations of miRNA mimics and luciferase activity was evaluated in cell lysates 48 h later.
340 The fold change of *Renilla/*firefly luciferase signal was normalized to a control group
341 containing either a non-targeting siRNA or a miRNA mimic without a predicted binding site
342 in the 3'UTR fragment of the target gene.

343 The first gene we investigated, *Neurod1*, is an important transcription factor regulating
344 neuronal differentiation and migration in the developing cerebral cortex (39). *Neurod1* contains
345 binding sites for miR-137-3p and miR-153-3p that were previously demonstrated to co-
346 operatively repress the gene's expression (20). Therefore, we used this experiment as a positive
347 control. We independently cloned two *Neurod1* 3' UTR fragments with different lengths (274
348 bp and 1188 bp, respectively). The luciferase activity was significantly reduced in cells
349 transfected with the combination of miR-137-3p and miR-153-3p compared to individual
350 miRNAs as well as two different negative controls (siRNA and miR-128-3p), thereby
351 confirming the co-targeting effect previously observed (Fig 6A-B).
352 *Src*, a proto-oncogene that codes for a non-receptor protein tyrosine kinase is another important
353 neurodevelopmental regulator that contains binding sites for both miR-137-3p and miR-153-3p in
354 its 3'UTR. *Src* is expressed at steadily high levels in the mouse neocortex from E12.5 to P1 and
355 overexpression of this gene leads to impaired neuronal migration due to altered adhesion properties
356 and cytoskeletal dynamics (40). We observed that the combination of both miRNAs exerted a
357 significantly stronger repressive effect on *Src* compared to each individual miRNA (Fig 6C).
358 As an additional target gene for the reporter assays, we selected *Cxcl12* which is also an important
359 regulator of early brain development. *Cxcl12* is involved in migration of NPCs, early localization
360 of Cajal-Retzius cells in the developing cortex, and in axon guidance and pathfinding (41, 42).
361 *Cxcl12* is a predicted target of miR-137-3p and miR-135b-5p. Luciferase reporter assays showed
362 that co-transfection with both miRNAs significantly increased the repressive effect compared to
363 the negative siRNA control and treatment with each miRNA separately (Fig 6D).
364

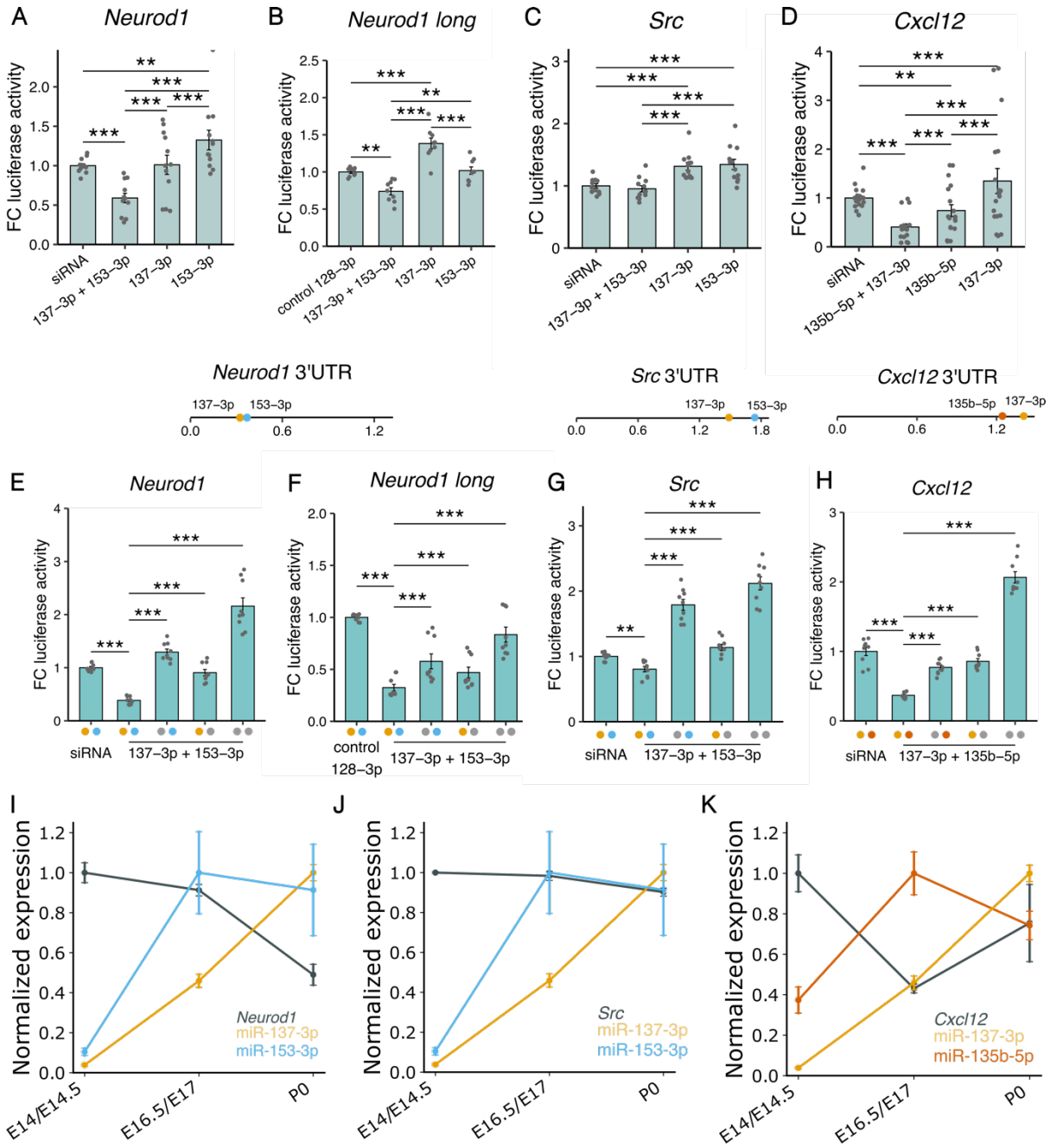

Fig. 6 Luciferase activity in lysates of HEK293 cells transfected with plasmids containing 3' UTR fragments of target genes. A-D Lysates were co-transfected with different combinations of miRNA mimics. Fold change (FC) of luciferase activity was obtained by calculating the ratio of *Renilla* luciferase and firefly luciferase activity and then normalizing to the mean of the control siRNA or miRNA group. Locations of the binding sites in the 3' UTR of the respective gene are represented by colored dots. The length of the 3' UTRs is indicated in kbp. **E-H** Fold change of luciferase activity was measured after introducing point mutations in the binding sites of the miRNAs in the 3' UTR regions. Colored dots on the x-axis indicate that the binding site of the respective miRNA was intact, gray dots indicate a mutated binding site. **I-K** Expression of miRNAs and target genes during

374 embryonic brain development. Expression values were normalized to a 0-1 range. Target gene expression values
375 were measured at E14.5, E16.5 and P0 and were obtained from the study by Weyn-Vanhentenryck et al.(34). Data
376 are shown as mean ± standard error of the mean and individual values. *p<0.05, ** p<0.01, *** p<0.001, two-
377 way analysis of variance followed by Tukey's post-hoc test.
378
379 In contrast, we did not observe a significant co-targeting effect for miR-153-3p with miR-129-
380 5p and miR-137-3p with miR-128-3p in reporter assays with *Apc* and *Ndst1,* respectively (Fig
381 S5A, C). Furthermore, we aimed to investigate if higher-order co-targeting interactions,
382 including three miRNAs would exert stronger silencing effects on gene expression. To this
383 end, we co-transfected cells with plasmids containing the 3' UTR fragment of the *Dcx* gene
384 and mimics of miR-128-3p, miR-129-5p, and miR-135b-5p (Fig S5B). In an additional assay,
385 we cloned the 3' UTR of *Zeb2* and co-transfected cells with its targeting miRNAs – miR-129-
386 5p, miR-137-3p and miR-153-3p (Fig S5D). Treatment with different miRNA mimics
387 significantly reduced luciferase activity compared to the siRNA control in the *Zeb2* assays.
388 However, we did not observe a significant cooperative repressive effect for either *Dcx* or *Zeb2.*
389 To confirm that the cooperative silencing effect for *Neurod1, Src,* and *Cxcl12* was mediated
390 via direct binding of the miRNAs, we employed *in vitro* site-directed mutagenesis to introduce
391 mutations in the miRNA binding sites of the 3' UTRs. We generated plasmids carrying a
392 mutation in one of the binding sites or in both binding sites of the respective co-targeting pair.
393 For all three genes, we observed the highest luciferase activity in the cell lysates where both
394 miRNA binding sites were mutated. Conversely, the strongest repressive effect was detected
395 when both binding sites were intact, thereby confirming that miRNAs acted co-operatively to
396 exert stronger gene silencing (Fig 6E-H). Furthermore, we investigated the expression patterns
397 of these three genes by employing the data from Weyn-Vanhentenryck et al. (34). *Neurod1*
398 was significantly down-regulated at P0 compared to E14.5 and E16.5, correlating negatively
399 with the expression pattern of the co-targeting pair mir-137-3p and miR-153-3p (Fig 6I, Fig

400 S6A). While *Src* was not differentially regulated, it still had its expression minimum at P0 (Fig
401 6J, Fig S6B). Interestingly, *Cxcl12* had a significantly reduced expression only at E16.5
402 compared to E14.5, but this pattern negatively correlated with the expression peak of miR-
403 135b-5p at E17 (Fig 6K, Fig S6C). These matching *in vivo* expression patterns of the miRNAs
404 and the genes they co-target lend further support to the biological relevance of the co-operative
405 miRNA gene silencing we observed in the luciferase assays.
406

407 **Discussion**

408 Our study provides a detailed map of the longitudinal changes in miRNA expression patterns
409 that occur in the transition between NPCs and neurons as well as *in vivo* at key stages of
410 embryonic cortical development in the mouse. Previous studies employing high-throughput
411 sequencing to examine miRNA composition in the embryonic cortex have focused on a single
412 time point (29, 43). In contrast, *in situ* hybridization-based technologies have successfully
413 profiled miRNA expression in different embryonic brain structures and at multiple time points
414 (44), however, this analysis has been limited to a pre-selected set of miRNAs. To our
415 knowledge, this is the first high-throughput longitudinal investigation, therefore providing a
416 valuable resource for elucidating the regulatory role miRNAs play during embryonic
417 corticogenesis.
418 Remarkably, the majority of the miRNAs significantly altered their expression level already at
419 the transition from E14 to E17. This predominantly neurogenic phase is characterized by a
420 complex interplay of multiple processes that shape late-stage embryonic corticogenesis (45).
421 At E14, radial glia cells in the ventricular zone have switched from symmetrical to
422 asymmetrical divisions to give rise to the basal progenitors that later generate neurons.
423 Subsequently, newly born neurons migrate out of the ventricular zone to the upper layers of
424 the neocortex where they differentiate into mature neurons. Upon neurogenesis completion at

425 around E17, neural stem cells give rise to the other brain cell types including astrocytes and
426 oligodendrocytes (28, 30). Cell fate commitment and neuronal identity are determined by
427 specialized transcriptional programs that occur in sequential waves and eventually result in the
428 immense cell type diversity observed in the brain (46, 47). The dynamic changes of miRNA
429 expression we detected indicate that miRNA networks can act as quick regulators of these
430 transcriptional programs by controlling the expression of cell-type specific genes (48).
431 miRNA-mediated transcriptional inhibition could also contribute to reducing excess levels of
432 target mRNA arising as noise from transcriptional bursts and thereby ensuring appropriate cell-
433 type or developmental-stage specific expression.
434 By employing a co-expression network analysis, we detected sets of co-regulated miRNAs
435 with individual miRNAs acting as hubs at early (e.g., miR-92a/b) and late (e.g., miR-124 and
436 miR-137) stages of neurogenesis. miR-92 is a part of the miR-17-92 cluster that is involved in
437 the maintenance of neural stem cells, and its genetic ablation results in a reduced pool of neural
438 stem and radial glia cells and a premature transition to intermediate progenitors (49).
439 Furthermore, miR-137 has been reported previously to influence neuronal differentiation via a
440 regulatory loop between TLX and miR-137' downstream target LSD1 (50).
441 Interestingly, we observed an enrichment of down-regulated genes at P0 compared to E14,
442 which were validated targets of hub miRNAs in the green module (Fig 3E). This module
443 consisted of miRNAs that were up-regulated at P0. A GO annotation analysis revealed that
444 many of these genes are regulators of key processes that are responsible for keeping neural
445 stem cells in a proliferative state and blocking neuronal differentiation. For instance, the
446 canonical NPC marker *Sox2* is crucial for the maintenance and self-renewal of progenitors (51,
447 52), and silencing its expression promotes neuronal differentiation (51). Another member of
448 the SOX transcription factor family – *Sox9,* also plays an important role in maintaining neural
449 stem cells in the early embryonic neocortex and its expression levels determine self-renewal

450 and neurogenic division behavior of radial glial cells (53) . In fact, a recent review highlighted
451 a complex regulatory interplay between SOX transcription factors and miRNAs that guide
452 distinct cellular activities in the developing and adult brain under physiological and
453 pathological conditions (54).
454 Green module hub miRNA targets that were down-regulated at P0 also included positive
455 regulators of Notch signaling and negative regulators of the Wnt pathway. Activation of the
456 Notch pathway indeed leads to maintaining the neural progenitor pool (55). Furthermore,
457 inhibiting Wnt signaling during mid and late stages of neurogenesis in the neocortex was
458 previously reported to result in reduced neuronal production (56).
459 Another crucial mechanism through which miRNAs can influence the development of the
460 cerebral cortex is via the regulation of RNA-binding proteins. In line with this, we observed
461 that several effectors of alternative splicing whose expression significantly changed during
462 embryonic corticogenesis were validated targets of hub miRNAs (Fig 3F). Alternative splicing
463 plays a pivotal role in neuronal differentiation (57), axonogenesis (58) and synapse formation
464 (59). In this context, miR-124 represents one of the most well-studied examples in neuronal
465 differentiation. miR-124 targets PTBP1, a protein that represses neuronal splice patterns. The
466 upregulation of miR-124 in neurons is sufficient to suppress the expression of *Ptbp1* and
467 thereby induce the necessary splicing changes for the transition from NPCs to neurons (36).
468 Thus, miRNAs could act as a post-transcriptional mechanism ensuring the precise spatio-
469 temporal expression of RNA-binding proteins which is critical for proper development of the
470 central nervous system (60).
471 Surprisingly, the gene silencing effect of most miRNAs is modest despite their crucial
472 regulatory potential (61), indicating that – with the exception of hub miRNAs – they might be
473 fine tuners rather than master regulators of embryonic brain development. However, the
474 redundancy of multiple co-expressed miRNAs sharing the same target genes supports the

475 mechanism of co-operative binding to enhance the gene-silencing effect of individual miRNAs
476 (20). Accordingly, we confirmed the co-targeting for several neurodevelopmentally relevant
477 genes in luciferase assays (Fig. 6). Furthermore, the negative correlation between the *in vivo*
478 miRNA and target expression peaks strongly suggests that co-targeting is a biological
479 phenomenon that can occur during embryonic cortical development. As 3' UTRs of mRNAs
480 expressed in the brain are longer compared to other tissues (62) and this length even increases
481 in neuronal transcripts (63), the brain indeed offers extremely favorable conditions for the
482 emergence of miRNA multi-targeting networks (20).
483 Notably, significant co-targeting relationships between co-expressed miRNAs were as likely
484 as co-targeting associations between miRNAs regulated in opposite directions. Apart from
485 simultaneous cooperative biding to enhance gene silencing, this observation points to an
486 alternative evolutionary need for the presence of multiple binding sites for distinct miRNAs in
487 the same gene, namely regulating the expression at different time points or in diverse cell types.
488 Accordingly, Nowakowski and colleagues recently reported cell-type specific miRNA-mRNA
489 interactions in the developing human cortex using a single-cell profiling strategy (48). Thus,
490 distinct miRNAs might be responsible for silencing temporally or spatially abnormal
491 expression of an overlapping set of genes. This explains our observation of miRNAs with
492 opposite expression patterns that share more targets than expected by chance.
493 In summary, we detected dynamic changes in miRNA expression during embryonic brain
494 development with distinct miRNAs acting as hubs in co-expression and co-targeting networks.
495 Furthermore, we showed that miRNAs might be particularly important for controlling cell fate
496 commitment and neuronal differentiation by silencing the expression of genes that promote
497 neural stem cell proliferation and maintenance as well as NPC-like splicing patterns. Our study
498 also provides additional evidence that simultaneous binding to common targets increases the
499 transcriptional repression effect of miRNAs. To further resolve the complexity of mRNA-

500 miRNA as well as miRNA co-targeting networks in distinct cell types *in vivo,* future studies
501 should focus on single-cell high-throughput profiling techniques.
502

503 ## Methods

504 **miRNA sequencing of the developing mouse cerebral cortex and in NPCs/neurons**

505 For NPC/neuron culture, the cortices of E14.5 NMRI embryos (Janvier Labs; Le Genest-Saint-
506 Isle, France) were dissected and collected in cooled DMEM high glucose media (Gibco Life
507 Technologies) and processed into single cells by trypsin digestion. For NPC and neuron
508 culture, 0.2x10^6 cells per well and 1.4x10^6 cells per well, respectively, were seeded on Poly-
509 L-ornithin and Laminin coated 6 well plates. The NPCs were cultured in neurobasal medium
510 containing 2% B27 -VitA supplement (Gibco Life Technologies), 500µM Glutamax (Gibco
511 Life Technologies) and EGF (10ng/ml) and FGF (10ng/ml). For neural differentiation, the cells
512 were cultured in neurobasal medium containing 2% B27 supplement (Gibco Life
513 Technologies) and 500 µM Glutamax (Gibco Life Technologies). Total RNA, including
514 miRNA, was isolated from the NPCs and neurons as well as from cortices of female and male
515 NMRI embryos (Janvier Labs; Le Genest-Saint-Isle, France) at the time points E14, E17 and
516 P0 (n=6 embryos per sex and time point) using the Qiagen miRNeasy mini kit (CatNo. 217004;
517 Qiagen; Hilden, Germany). 500 ng of total RNA, including miRNA, were used as an input for
518 library preparation with the Bioo Scientific NextFlex small RNA v3 Seq Kit (CatNo. NOVA-
519 5132-05; Bioo Scientific; Austin, USA). Library preparation was conducted according to the
520 kit manual. Size distribution and concentrations of the prepared libraries were checked by
521 Qubit dsDNA High Sensitivity Assay (CatNo. Q32851; Thermo Scientific; Waltham, USA).
522 0.5 nanomoles (NPCs/neurons) or 4 nanomoles (Cortex samples) of the prepared miRNA
523 libraries were loaded on a High Output v2 kit (75 cycles) Illumina cartridge which was run on
524 a NextSeq 500 device.

525

526 **miRNA sequencing data pre-processing**

527 After the sequencing, bcl2fastq v2.17.1.14 conversion software (Illumina, Inc.) was used to
528 demultiplex sequencing data and convert base call (BCL) files into fastq files. The trimming
529 of the fastq files was conducted in two steps as suggested by the NEXTflex™ Small RNA
530 Trimming Instructions. Briefly, sequencing adapters (TGGAATTCTCGGGTGCCAAGG)
531 were trimmed and reads shorter than 15 nucleotides were removed from further analysis.
532 Afterwards, 4 bases from either side of each read were trimmed using Cutadapt v1.18. Quality
533 control checks were performed on the trimmed data with FastQC v0.11.7.

534

535 **miNRA differential expression analysis**

536 miRNA samples with at least 20 million reads were further analyzed. Using miRDeep's
537 v2.0.1.2 *mapper.pl* script, miRNA reads were mapped to the *Mus musculus* GRCm38 genome.
538 Afterwards, known and novel miRNA were identified using the *miRDeep2.pl* script. Prior to
539 differential expression analysis, miRNAs with CPM expression values less than 10 were
540 filtered out using edgeR v3.30.3. Differential expression analysis was then performed with
541 DESeq2 v1.28.1. miRNAs with an adjusted p-value <0.05 and an absolute log fold change
542 exceeding 0.5 were considered differentially expressed. P-values were corrected for multiple
543 comparisons with the Benjamini-Hochberg method.

544

545 **Weighted gene co-expression network analysis**

546 We performed a Weighted Correlation Network Analysis (WGCNA) (33) to find clusters or
547 "modules" of co-expressed miRNAs. For the analysis, a *bicor* correlation type and a *signed*
548 network type with soft-thresholding power of 24, minimal module size of 5 and dynamic tree
549 cut height of 0.2 were applied. Target prediction of the miRNAs in each module was performed

using the TargetScanMouse database v7.2 (64). Functional enrichment analysis of the different modules in the co-expression network was conducted using the clusterProfiler v4.6.2 R package and the target genes of the miRNAs in the respective module as input.

Key driver analysis

To identify hub (or key driver) miRNAs in the modules of the co-expression network, we performed a key driver analysis as previously described (31, 32). First, we used the algorithm for the reconstruction of cellular networks (ARACNE) (65) as implemented in the bnlearn R package v4.8.3 to obtain an undirected gene regulatory network from the expression levels of the miRNAs in the respective WGCNA module. Next, we performed key driver analysis on the ARACNE reconstructed network using the KDA R package v0.2.2 (https://github.com/mw201608/mnml-public/tree/master/pkgs) to identify important regulatory miRNAs.

Analysis of publicly available RNA-seq data of the developing mouse cortex

To explore the expression of target genes during cortical development, we re-analyzed publicly available data from the study by Weyn-Vanhentenryck et al.(34) containing RNA-seq of the mouse cortex. We focused on E14.5, E16.5, P0 as these were comparable with the time points in our study. Fastq files were downloaded from the NCBI Short Read Archive, accession number SRP055008. After trimming with BBDuk v39.01, reads were mapped to the Gencode mm39 reference genome (released 19.10.2022) using STAR v2.7.10b. A count matrix was obtained using FeatureCounts provided by SubRead v2.0.6. Differential expression analysis was performed with DESeq2 v1.40.1 with default settings. Genes with an adjusted p-value (Benjamini-Hochberg method) < 0.05 were considered to be differentially expressed.

575 **miRNA expression profiling using RT-qPCR**

576 miRNA expression patterns identified by small RNA sequencing were validated with the
577 TaqMan MicroRNA Assay (Applied Biosystems). Reverse transcription was performed using
578 the TaqMan MicroRNA Reverse Transcription Kit (Applied Biosystems; CatNo. 4366596).
579 RT-qPCRs were conducted with the TaqMan Universal Master Mix II, no UNG (Applied
580 Biosystems; CatNo. 4440040) on a StepOnePlus Real-Time PCR System (Applied
581 Biosystems). The U6 snRNA was used as a control for normalization of experimental samples.
582 Relative quantification (RQ) values of miRNA expression were calculated with the ΔΔCT
583 method. Expression levels in NPCs and E14 samples, respectively, were used as reference
584 groups. Primers used for the RT-qPCR analysis are shown in Table S1.

585

586 **miRNA co-targeting prediction**

587 miRNA co-targeting analysis was performed using a custom R script. We employed the
588 TargetScanMouse database v7.2 to identify the broadly conserved mRNA targets for each
589 miRNA. miRNAs which belong to the same broadly conserved family and therefore have
590 identical gene target sets were grouped together for further analysis. Additionally, we only kept
591 miRNAs with at least 300 targets (20).

592 Subsequently, we created a custom control set for each miRNA, containing genes with similar
593 3' UTR length, GC content, and sequence conservation as the actual genes included in the
594 respective target set based on a case-control strategy. To select the best matching control for a
595 gene *X* from the respective target set (case), first we filtered the potential pool of candidates
596 for genes with a 3' UTR length within the range of 0.85-1.15 of the 3'UTR length of target
597 gene *X.* Then, we filtered out genes with a GC content outside the range of 0.95-1.05 of the
598 GC content of gene *X*. Finally, we eliminated candidates with a phyloP score outside the range
599 of 0.8-1.2 for gene *X.* If more than one candidate remained after the filtering steps, a control

600 gene *Y* for the target gene *X* was picked randomly. If the filtering steps returned an empty set,
601 no control gene was selected for the respective target. This procedure was repeated for all genes
602 included in the target set for the miRNA. The filtering cut-off values were selected empirically
603 to maximize the number of controls while simultaneously minimizing the difference in the 3'
604 UTR length, GC content, and phyloP score distributions of genes in the target and control sets.
605 The similarity of the distributions of the three parameters between the control and target sets
606 was ensured by non-significant pairwise Wilcoxon tests.
607 We considered miRNA *A* and miRNA *B* to be a co-targeting pair if the intersection of their
608 target sets contained more genes than what would be expected by chance. To this end, we
609 compared the observed number of common targets with the expected number obtained by
610 intersecting the target set of miRNA *A* with the control set of miRNA *B* and vice versa. This
611 yields two comparisons for each pair of miRNAs whose significance was evaluated with a
612 Fisher's exact test. If both tests were statistically significant after a false discovery rate p-value
613 adjustment (Benjamini-Hochberg method), then we considered miRNA *A* and miRNA *B* to be
614 a bidirectional co-targeting pair. To quantify the magnitude of the co-targeting relationship, we
615 calculated the odds ratios with values significantly higher than 1 corresponding to a pair of
616 miRNAs sharing a significantly higher number of targets than what would be expected by
617 chance. Higher odds ratios indicate a higher number of shared targets. To ensure that co-
618 targeting pairs do not originate from identical seed sequences, miRNAs having identical seeds
619 up to one mismatch were excluded *a priori* from the statistical analysis.
620
621 **Comparing the number of intra- and inter-modular co-targeting relationships**
622 To investigate if the black or green WCGNA modules contain more intra-modular (miRNAs
623 of the same module) than inter-modular (miRNAs from different modules) co-targeting
624 relationships, we performed a Fisher's exact test on the following contingency table:

	Significant co-targeting relationship	Non-significant co-targeting relationship
Intra-modular	m	M - m
Inter-modular	n	N - n

625 where *m* represents the number of significant intra-modular co-targeting relationships, *M*
626 corresponds to the total number of possible intra-modular relationships, *n* corresponds to the
627 number of significant inter-modular relationships and *N* refers to the total number of possible
628 inter-modular relationships. We used the following formula to calculate *M*:

629 $$M = x(x-1)/2$$

630 where *x* corresponds to the number of miRNAs in the respective module. The total number of
631 possible inter-modular relationships was estimated with the formula:

632 $$N = xy$$

633 with *x* being the number of miRNAs in the module of interest and *y* corresponding to the
634 number of miRNAs in the remaining modules.

635

636 **Luciferase reporter assays**

637 3' UTR fragments of miRNA target genes (for primer sequences see Table S2) were cloned
638 into the XhoI/NotI sites downstream of the synthetic *Renilla* luciferase gene of psiCHECK-2
639 vector (Promega; CatNo. C8021). Mutations in the miRNA binding sites were introduced using
640 the QuikChange II XL system (Agilent Technologies; CatNo. 200521-5). Primers used are
641 shown in Table S2. $5x10^4$ HEK293 cells were seeded into each well of a 12-well plate. 24
642 hours later, 200 ng psiCHECK-2 reporter plasmid were co-transfected with 5 µl miScript
643 miRNA mimics (Qiagen; CatNo. 219600) using 4 µl Lipofectamine 2000 Transfection Reagent
644 (Thermo Fisher Scientific; CatNo. 11668019). Luciferase reporter assays were conducted 48

645 hours later using the Dual-Luciferase Reporter Assay System (Promega; CatNo. E1980).
646 Luciferase activity was measured on a CentroXS LB 960 (Berthold Technologies).
647

648 **Statistical analysis of qPCR and luciferase reporter assay data**

649 Two groups were compared statistically using an unpaired t-test or Welch's t-test in case of
650 unequal variance between groups. For comparisons of three groups, a one- or two-way analysis
651 of variance (ANOVA) followed by Tukey's post hoc test was performed. The assumptions of
652 the linear model were evaluated by inspecting Q-Q plots and fitted values vs. residuals plots.
653 Relative quantification values from the RT-qPCR assays were $\log_e$-transformed prior to
654 statistical testing. All p-values are two-tailed and a p-value ≤ 0.05 was considered statistically
655 significant. Statistical analysis was performed using R v. 4.2.2.

656 **Ethics statement**

657 Ethical review and approval were not required for the animal study because the study did not
658 include any animal experiments requiring approval. To carry out this study, mice were killed
659 for organ removal. In Germany, this procedure is notifiable but does not require approval by
660 an ethics committee.

661 **Competing interests**

662 The authors declare they have no competing interests.

663 **Acknowledgements**

664 HT and SG acknowledge funding by the Landesinitiative Rheinland-Pfalz and the Resilience,
665 Adaptation, and Longevity (ReALity) initiative of the Johannes Gutenberg University of
666 Mainz. SW was funded by the Emergent Algorithmic Intelligence initiative of the Johannes
667 Gutenberg University Mainz supported by the Carl-Zeiss foundation. JW acknowledges
668 funding from the Deutsche Forschungsgemeinschaft (WI-3837 / 8-1).

669 **Author contributions**

670 HT, DH and SW performed the bioinformatics analysis. LS and HM performed miRNA
671 sequencing, RT-qPCR and luciferase experiments. HT and JW wrote the manuscript. SG and
672 JW supervised the study. All authors read and approved the final version of the manuscript.

673 **Data availability**

674 The raw RNA-seq data were uploaded to the Sequence Read Archive (SRA) data base under
675 the accession number PRJNA1018560.

676 The following supplementary tables are available online under 10.5281/zenodo.1016183:

677 Supplementary_table_1.xlsx: Differentially expressed miRNAs between E14, E17 and P0
678 cortical samples as well as NPCs versus neurons

679 Supplementary_table_2.xlsx: Module assignment of miRNAs in the WCGNA analysis.

680 Supplementary_table_3.xlsx: GO terms of miRNA targets of the black and green modules from
681 the WCGNA analysis.

682 Supplementary_table_4.xlsx: Significant co-targeting relationships between miRNAs/miRNA
683 families.

684 References

685 1. Lee Y, Kim M, Han J, Yeom KH, Lee S, Baek SH, et al. MicroRNA genes are transcribed
686 by RNA polymerase II. EMBO J. 2004;23(20):4051-60.
687 2. Borchert GM, Lanier W, Davidson BL. RNA polymerase III transcribes human
688 microRNAs. Nat Struct Mol Biol. 2006;13(12):1097-101.
689 3. Denli AM, Tops BB, Plasterk RH, Ketting RF, Hannon GJ. Processing of primary
690 microRNAs by the Microprocessor complex. Nature. 2004;432(7014):231-5.
691 4. Gregory RI, Yan KP, Amuthan G, Chendrimada T, Doratotaj B, Cooch N, et al. The
692 Microprocessor complex mediates the genesis of microRNAs. Nature. 2004;432(7014):235-
693 40.
694 5. Han J, Lee Y, Yeom KH, Kim YK, Jin H, Kim VN. The Drosha-DGCR8 complex in primary
695 microRNA processing. Genes Dev. 2004;18(24):3016-27.
696 6. Yi R, Qin Y, Macara IG, Cullen BR. Exportin-5 mediates the nuclear export of pre-
697 microRNAs and short hairpin RNAs. Genes Dev. 2003;17(24):3011-6.
698 7. Ketting RF, Fischer SE, Bernstein E, Sijen T, Hannon GJ, Plasterk RH. Dicer functions in
699 RNA interference and in synthesis of small RNA involved in developmental timing in C.
700 elegans. Genes Dev. 2001;15(20):2654-9.
701 8. O'Brien J, Hayder H, Zayed Y, Peng C. Overview of MicroRNA Biogenesis, Mechanisms
702 of Actions, and Circulation. Front Endocrinol (Lausanne). 2018;9:402.

703 9. Davis TH, Cuellar TL, Koch SM, Barker AJ, Harfe BD, McManus MT, et al. Conditional
704 loss of Dicer disrupts cellular and tissue morphogenesis in the cortex and hippocampus. J
705 Neurosci. 2008;28(17):4322-30.
706 10. McLoughlin HS, Fineberg SK, Ghosh LL, Tecedor L, Davidson BL. Dicer is required for
707 proliferation, viability, migration and differentiation in corticoneurogenesis. Neuroscience.
708 2012;223:285-95.
709 11. Kawase-Koga Y, Otaegi G, Sun T. Different timings of Dicer deletion affect
710 neurogenesis and gliogenesis in the developing mouse central nervous system. Dev Dyn.
711 2009;238(11):2800-12.
712 12. Nowakowski TJ, Mysiak KS, Pratt T, Price DJ. Functional dicer is necessary for
713 appropriate specification of radial glia during early development of mouse telencephalon.
714 PLoS One. 2011;6(8):e23013.
715 13. Saurat N, Andersson T, Vasistha NA, Molnar Z, Livesey FJ. Dicer is required for neural
716 stem cell multipotency and lineage progression during cerebral cortex development. Neural
717 Dev. 2013;8:14.
718 14. De Pietri Tonelli D, Pulvers JN, Haffner C, Murchison EP, Hannon GJ, Huttner WB.
719 miRNAs are essential for survival and differentiation of newborn neurons but not for
720 expansion of neural progenitors during early neurogenesis in the mouse embryonic
721 neocortex. Development. 2008;135(23):3911-21.
722 15. De Pietri Tonelli D, Clovis YM, Huttner WB. Detection and monitoring of microRNA
723 expression in developing mouse brain and fixed brain cryosections. Methods Mol Biol.
724 2014;1092:31-42.
725 16. Alles J, Fehlmann T, Fischer U, Backes C, Galata V, Minet M, et al. An estimate of the
726 total number of true human miRNAs. Nucleic Acids Res. 2019;47(7):3353-64.
727 17. Prieto-Colomina A, Fernández V, Chinnappa K, Borrell V. MiRNAs in early brain
728 development and pediatric cancer: At the intersection between healthy and diseased
729 embryonic development. Bioessays. 2021;43(7):e2100073.
730 18. Winter J. MicroRNAs of the miR379-410 cluster: New players in embryonic
731 neurogenesis and regulators of neuronal function. Neurogenesis (Austin).
732 2015;2(1):e1004970.
733 19. Rago L, Beattie R, Taylor V, Winter J. miR379-410 cluster miRNAs regulate
734 neurogenesis and neuronal migration by fine-tuning N-cadherin. EMBO J. 2014;33(8):906-
735 20.
736 20. Cherone JM, Jorgji V, Burge CB. Cotargeting among microRNAs in the brain. Genome
737 Res. 2019;29(11):1791-804.
738 21. Krek A, Grun D, Poy MN, Wolf R, Rosenberg L, Epstein EJ, et al. Combinatorial
739 microRNA target predictions. Nat Genet. 2005;37(5):495-500.
740 22. Nielsen CB, Shomron N, Sandberg R, Hornstein E, Kitzman J, Burge CB. Determinants
741 of targeting by endogenous and exogenous microRNAs and siRNAs. RNA. 2007;13(11):1894-
742 910.
743 23. Grimson A, Farh KK, Johnston WK, Garrett-Engele P, Lim LP, Bartel DP. MicroRNA
744 targeting specificity in mammals: determinants beyond seed pairing. Mol Cell.
745 2007;27(1):91-105.
746 24. Saetrom P, Heale BS, Snove O, Jr., Aagaard L, Alluin J, Rossi JJ. Distance constraints
747 between microRNA target sites dictate efficacy and cooperativity. Nucleic Acids Res.
748 2007;35(7):2333-42.

749 25. Doench JG, Sharp PA. Specificity of microRNA target selection in translational
750 repression. Genes Dev. 2004;18(5):504-11.
751 26. Wu S, Huang S, Ding J, Zhao Y, Liang L, Liu T, et al. Multiple microRNAs modulate
752 p21Cip1/Waf1 expression by directly targeting its 3' untranslated region. Oncogene.
753 2010;29(15):2302-8.
754 27. Loo L, Simon JM, Xing L, McCoy ES, Niehaus JK, Guo J, et al. Single-cell transcriptomic
755 analysis of mouse neocortical development. Nature Communications. 2019;10(1):134.
756 28. Mukhtar T, Taylor V. Untangling Cortical Complexity During Development. Journal of
757 Experimental Neuroscience. 2018;12:1179069518759332.
758 29. Ling K-H, Brautigan PJ, Hahn CN, Daish T, Rayner JR, Cheah P-S, et al. Deep
759 sequencing analysis of the developing mouse brain reveals a novel microRNA. BMC
760 Genomics. 2011;12(1):176.
761 30. Cadwell CR, Bhaduri A, Mostajo-Radji MA, Keefe MG, Nowakowski TJ. Development
762 and Arealization of the Cerebral Cortex. Neuron. 2019;103(6):980-1004.
763 31. Bagot RC, Cates HM, Purushothaman I, Lorsch ZS, Walker DM, Wang J, et al. Circuit-
764 wide Transcriptional Profiling Reveals Brain Region-Specific Gene Networks Regulating
765 Depression Susceptibility. Neuron. 2016;90(5):969-83.
766 32. Lorsch ZS, Hamilton PJ, Ramakrishnan A, Parise EM, Salery M, Wright WJ, et al. Stress
767 resilience is promoted by a Zfp189-driven transcriptional network in prefrontal cortex.
768 Nature Neuroscience. 2019;22(9):1413-23.
769 33. Langfelder P, Horvath S. WGCNA: an R package for weighted correlation network
770 analysis. BMC Bioinformatics. 2008;9(1):559.
771 34. Weyn-Vanhentenryck SM, Feng H, Ustianenko D, Duffié R, Yan Q, Jacko M, et al.
772 Precise temporal regulation of alternative splicing during neural development. Nature
773 Communications. 2018;9(1):2189.
774 35. Huang HY, Lin YC, Cui S, Huang Y, Tang Y, Xu J, et al. miRTarBase update 2022: an
775 informative resource for experimentally validated miRNA-target interactions. Nucleic Acids
776 Res. 2022;50(D1):D222-d30.
777 36. Makeyev EV, Zhang J, Carrasco MA, Maniatis T. The MicroRNA miR-124 promotes
778 neuronal differentiation by triggering brain-specific alternative pre-mRNA splicing. Mol Cell.
779 2007;27(3):435-48.
780 37. Jensen KB, Dredge BK, Stefani G, Zhong R, Buckanovich RJ, Okano HJ, et al. Nova-1
781 regulates neuron-specific alternative splicing and is essential for neuronal viability. Neuron.
782 2000;25(2):359-71.
783 38. Ule J, Ule A, Spencer J, Williams A, Hu JS, Cline M, et al. Nova regulates brain-specific
784 splicing to shape the synapse. Nat Genet. 2005;37(8):844-52.
785 39. Tutukova S, Tarabykin V, Hernandez-Miranda LR. The Role of Neurod Genes in Brain
786 Development, Function, and Disease. Frontiers in Molecular Neuroscience. 2021;14.
787 40. Wang JT, Song LZ, Li LL, Zhang W, Chai XJ, An L, et al. Src controls neuronal migration
788 by regulating the activity of FAK and cofilin. Neuroscience. 2015;292:90-100.
789 41. Li M, Ransohoff RM. Multiple roles of chemokine CXCL12 in the central nervous
790 system: a migration from immunology to neurobiology. Prog Neurobiol. 2008;84(2):116-31.
791 42. Mithal DS, Banisadr G, Miller RJ. CXCL12 signaling in the development of the nervous
792 system. J Neuroimmune Pharmacol. 2012;7(4):820-34.
793 43. Dori M, Cavalli D, Lesche M, Massalini S, Alieh LHA, de Toledo BC, et al. MicroRNA
794 profiling of mouse cortical progenitors and neurons reveals miR-486-5p as a regulator of
795 neurogenesis. Development. 2020;147(9).

796 44. Shu P, Wu C, Liu W, Ruan X, Liu C, Hou L, et al. The spatiotemporal expression
797 pattern of microRNAs in the developing mouse nervous system. Journal of Biological
798 Chemistry. 2019;294(10):3444-53.
799 45. Pilaz L-J, Silver DL. Post-transcriptional regulation in corticogenesis: how RNA-binding
800 proteins help build the brain. WIREs RNA. 2015;6(5):501-15.
801 46. Mukhtar T, Breda J, Adam MA, Boareto M, Grobecker P, Karimaddini Z, et al.
802 Temporal and sequential transcriptional dynamics define lineage shifts in corticogenesis.
803 Embo j. 2022;41(24):e111132.
804 47. Telley L, Govindan S, Prados J, Stevant I, Nef S, Dermitzakis E, et al. Sequential
805 transcriptional waves direct the differentiation of newborn neurons in the mouse
806 neocortex. Science. 2016;351(6280):1443-6.
807 48. Nowakowski TJ, Rani N, Golkaram M, Zhou HR, Alvarado B, Huch K, et al. Regulation
808 of cell-type-specific transcriptomes by microRNA networks during human brain
809 development. Nature Neuroscience. 2018;21(12):1784-92.
810 49. Bian S, Hong J, Li Q, Schebelle L, Pollock A, Knauss JL, et al. MicroRNA cluster miR-17-
811 92 regulates neural stem cell expansion and transition to intermediate progenitors in the
812 developing mouse neocortex. Cell Rep. 2013;3(5):1398-406.
813 50. Sun G, Ye P, Murai K, Lang MF, Li S, Zhang H, et al. miR-137 forms a regulatory loop
814 with nuclear receptor TLX and LSD1 in neural stem cells. Nat Commun. 2011;2:529.
815 51. Graham V, Khudyakov J, Ellis P, Pevny L. SOX2 Functions to Maintain Neural
816 Progenitor Identity. Neuron. 2003;39(5):749-65.
817 52. Hagey DW, Muhr J. Sox2 Acts in a Dose-Dependent Fashion to Regulate Proliferation
818 of Cortical Progenitors. Cell Reports. 2014;9(5):1908-20.
819 53. Fabra-Beser J, Alves Medeiros de Araujo J, Marques-Coelho D, Goff LA, Costa MR,
820 Müller U, et al. Differential Expression Levels of Sox9 in Early Neocortical Radial Glial Cells
821 Regulate the Decision between Stem Cell Maintenance and Differentiation. J Neurosci.
822 2021;41(33):6969-86.
823 54. Stevanovic M, Stanisavljevic Ninkovic D, Mojsin M, Drakulic D, Schwirtlich M.
824 Interplay of SOX transcription factors and microRNAs in the brain under physiological and
825 pathological conditions. Neural Regen Res. 2022;17(11):2325-34.
826 55. Imayoshi I, Sakamoto M, MasahiroYamaguchi, Mori K, Kageyama R. Essential Roles
827 of Notch Signaling in Maintenance of Neural Stem Cells in Developing and Adult Brains. The
828 Journal of Neuroscience. 2010;30(9):3489.
829 56. Munji RN, Choe Y, Li G, Siegenthaler JA, Pleasure SJ. Wnt signaling regulates
830 neuronal differentiation of cortical intermediate progenitors. J Neurosci. 2011;31(5):1676-
831 87.
832 57. Zhang X, Chen MH, Wu X, Kodani A, Fan J, Doan R, et al. Cell-Type-Specific
833 Alternative Splicing Governs Cell Fate in the Developing Cerebral Cortex. Cell.
834 2016;166(5):1147-62.e15.
835 58. Zhang M, Ergin V, Lin L, Stork C, Chen L, Zheng S. Axonogenesis Is Coordinated by
836 Neuron-Specific Alternative Splicing Programming and Splicing Regulator PTBP2. Neuron.
837 2019;101(4):690-706.e10.
838 59. Lin YS, Wang HY, Huang DF, Hsieh PF, Lin MY, Chou CH, et al. Neuronal Splicing
839 Regulator RBFOX3 (NeuN) Regulates Adult Hippocampal Neurogenesis and Synaptogenesis.
840 PLoS One. 2016;11(10):e0164164.
841 60. Vuong CK, Black DL, Zheng S. The neurogenetics of alternative splicing. Nature
842 Reviews Neuroscience. 2016;17(5):265-81.

843 61. Linsen SEV, Tops BBJ, Cuppen E. miRNAs: small changes, widespread effects. Cell
844 Research. 2008;18(12):1157-9.
845 62. Ramsköld D, Wang ET, Burge CB, Sandberg R. An abundance of ubiquitously
846 expressed genes revealed by tissue transcriptome sequence data. PLoS Comput Biol.
847 2009;5(12):e1000598.
848 63. Miura P, Shenker S, Andreu-Agullo C, Westholm JO, Lai EC. Widespread and
849 extensive lengthening of 3' UTRs in the mammalian brain. Genome Res. 2013;23(5):812-25.
850 64. Agarwal V, Bell GW, Nam J-W, Bartel DP. Predicting effective microRNA target sites
851 in mammalian mRNAs. eLife. 2015;4:e05005.
852 65. Margolin AA, Nemenman I, Basso K, Wiggins C, Stolovitzky G, Favera RD, et al.
853 ARACNE: An Algorithm for the Reconstruction of Gene Regulatory Networks in a
854 Mammalian Cellular Context. BMC Bioinformatics. 2006;7(1):S7.
855